Rocketdyne Division
Rockwell International

ASR74-388

SPACE SHUTTLE MANEUVERING ENGINE
REUSABLE THRUST CHAMBER PROGRAM
NAS9-12802

NASA CR-
141674

Task XI

High ε Injector Test Report

December 1974

Prepared by

R. P. Pauckert
SS/OME Principal Engineer
Advanced Projects

Approved by

R. D. Paster
Acting Program Manager
SS/OME Program

ROCKETDYNE DIVISION, ROCKWELL INTERNATIONAL
6633 Canoga Avenue
Canoga Park, California 91304

INTRODUCTION

The like-doublet element type injector is one of the candidates for the Space Shuttle Orbit Maneuvering Engine Thrust Chamber. Rocketdyne has conducted extensive tests with an 8-inch diameter like-doublet injector (L/D #1) to demonstrate moderately high performance and good thermal and stability characteristics (Task IX). A subscale injector test program conducted under the contract indicated the performance could be improved by increasing the interelement spacing (Task VI). Dimensional constraints on the 8-inch diameter configuration would have resulted in significant reduction in the number of elements which could be placed in the injector. Increasing the diameter to 10 inches significantly relaxes those constraints.

Although increasing the thrust chamber diameter lowers the resonant frequencies of tangential and radial modes, the reduced propellant mass flux tends towards a more stable condition. Regenerative cooling of the larger diameter chamber can be accomplished with a slightly lower pressure because of the lower predicted heat fluxes. These potential advantages of the larger diameter could only be verified through an experimental test program.

Specific test objectives are: 1) to determine performance and heat flux profiles vs chamber pressure and propellant mixture ratio; and 2) to determine stability characteristics with various acoustic cavity configurations.

The test program and results are described in this report.

SUMMARY

A total of 28 hot-fire tests were conducted with the 10-inch diameter L/D #4 injector. Operating conditions (chamber pressure, mixture ratio, and fuel temperature) were varied. Two chamber lengths and three acoustic cavity configurations were tested.

The injector was found to be stable with 10 and 15 percent area full-depth 1T cavities. The cavities had a contoured entrance without overlap between the chamber wall and the inner wall of the cavity. The injector was bombed unstable when the 15 percent area cavity was reduced to an effective depth of 1.28 inches. Heat flux profiles were low enough so that supplementary fuel boundary layer coolant is not required. The C* efficiency based on thrust was approximately 95% at nominal conditions with a 16-inch chamber length.

DISCUSSION

TEST HARDWARE

The test hardware consisted of the L/D #4 injector, a fuel distribution manifold, a solid wall-thrust chamber and cylindrical extensions, and replaceable acoustic cavity rings.

The L/D #4 injector is shown in Fig. 1. Injector characteristics are shown in Table 1. The injector was fabricated without supplementary fuel BLC orifices. Three radial baffles are incorporated into the fuel manifold of the injector to suppress coupling of acoustic and hydraulic oscillations.

The fuel manifold shown in Fig. 2 serves to distribute the fuel, simulating the regenerative thrust chamber coolant discharge. The manifold also retains the acoustic cavity rings in the same manner as the 8-inch diameter hardware described in the (Low ϵ Stability Test Report," ASR74-302. With this configuration, the acoustic cavities are formed by the injector and the replaceable two-piece cavity rings (Fig. 3). The aft ring defines the inlet geometry of the cavity and can be replaced with a new ring to provide a different inlet geometry without machining the forward ring. The forward ring defines the cavity width and depth. Only the forward ring need be modified to change the cavity depth. The rings are pinned together and to the fuel manifold to assure consistent orientation. Only the 10 and 15 percent area contoured inlet were tested.

The solid-wall thrust chamber shown in Fig. 4 has 3 bomb ports and 24 thermal isolation areas formed by trepanning circular grooves partially through the wall of the chamber. Thermocouples attached to the wall at these points provide temperature transient data to determine essentially one-dimensional heat flux values. Three ports are provided for measurement of chamber pressure with high frequency Kistel (Model 614B/644) transducers. The ports are located

Page intentionally left blank

Page intentionally left blank

Page intentionally left blank

Page intentionally left blank

TABLE 1

L/D #4 INJECTOR PARAMETERS

Injector Material	321 CRES
Face Diameter, inches	10.0
Type of Element	Like-doublet
Number of Elements	229
Diameter of fuel Element, inches	0.0294
Diameter of Oxidizer Element, inches	0.0309
O-F Element Spacing, inches	0.45
Cant Angle, degrees	4.5
Nominal Fuel ΔP, psi	45
Nominal Oxidizer ΔP, psi	55
Stabilization	Acoustic Cavities and Fuel Manifold Dams

2.7 inches from the injector face at angles of 12,108, and 228 degrees relative to the fuel inlet.

The 4-inch long chamber extension shown in Fig. 5 has the same bomb and pressure ports as the thrust chamber. The distance from the injector face to the throat of the assembly, including the extension, is 12 inches. An additional extension, similar to that shown in Fig. 5. but uninstrumented, was made to increase the injector-to-throat distance to 16 inches.

TEST FACILITY

The tests were conducted at the Victor Test Stand of the Rocketdyne Propulsion Research Area at Santa Susana where testing of the 8-inch hardware was just completed. A schematic of the feed system is shown in Fig. 6. NTO and MMH was supplied from pressurized tanks having maximum pressure capabilities of 2500 and 1500 psia, respectively. The oxidizer flows to the engine at ambient temperature.

The MMH is batch heated in the quantities required for a single firing through the use of a 4.5 gallon heat exchanger (limited to 430 psia) located upstream of the main fuel valve. In this heat exchanger, hot water flows inside four concentric coils of one-quarter-inch O.D. stainless tubing and provides a temperature limited heat source for the fuel. The fuel line from the heater to the main fuel valve has a hot water jacket. The heating water is circulated in a closed system from a steel reservoir tank through 2.5 gpm Burke pump, past an 18 kilowatt Chromalox electrical heater, and then through either the heat exchanger or a bypass loop back to the reservoir. An alternate supply of cold water can be introduced into the system to quickly cool the heat exchanger between tests and, thus, permit test personnel to work in the immediate vicinity of the heater test stand.

Page intentionally left blank

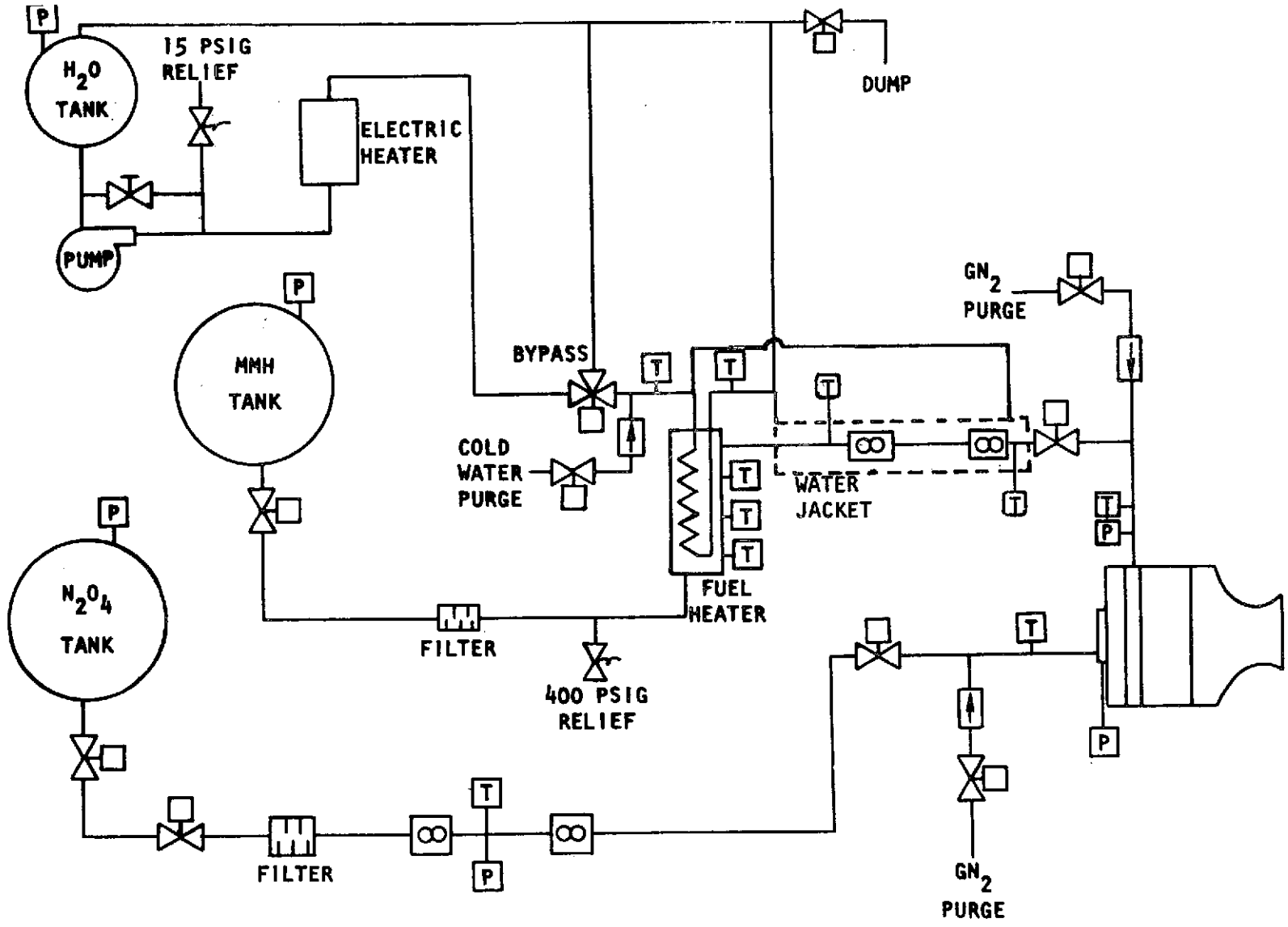

Figure 6. Propellant Feed System and Instrumentation Schematic

The NTO and MMH pass through 40μ filters before entering the engine valves. GN_2 purges are supplied downstream of the engine valves.

INSTRUMENTATION

High response pressure pickups were used to monitor chamber and injection pressures. Three Kistler transducers were mounted in the cylindrical spool approximately 2.7 inches from the injector face at 48, 192, and 288 degrees locations relative to the inlet of the fuel manifold viewing from aft to forward. The steady-state values of chamber pressure were measured using two Taber type transducers with sensing ports located in the acoustic cavities. These same type transducers were used to measure steady-state values of the fuel and oxidizer injection pressure and the feed system pressures. The temperature of the gas in the acoustic cavities were measured using tungsten/rhenium thermocouples. Chromel/alumel thermocouples were used to measure the thrust chamber wall temperatures. Propellant feed system temperatures were measured with iron/constantan thermocouples. Two turbine flow meters were used to measure each propellant flowrate. Thrust was also measured for computation of c*. The instrumentation is listed in Table 2. The estimated precision of each of the critical measurements (thrust, chamber pressure, and flowrate) is 0.25 percent.

High response data were recorded on tape and oscillograph. The oscillograph were also used to record the slower responding chamber pressure measurements, the flowrates, and the injection pressures. Most data except the high speed data were recorded on a digital tape. Direct inking charts were used to provide quick-look data.

TABLE 2

INSTRUMENTATION LIST FOR HIGH ε TEST PROGRAM

PARAMETER/MEASUREMENT	SYMBOL	TRANSDUCER EMPLOYED	RECORDING SYSTEM			
			BECKMAN DIGITAL DATA SYSTEM	DIRECT READING RECORDER	OSCILLO-GRAPH	TAPE
MMH (FUEL) SYSTEM						
MMH TANK PRESSURE	PFT	TABER		X		
FUEL FLOWRATE #1	WF-1	TURBINE FLOWMETER	X	X	X	
FUEL FLOWRATE #2	WF-2	TURBINE FLOWMETER	X	X	X	
FUEL FLOWMETER UPSTREAM TEMP.	TFL-1	I/C TC*	X	X		
FUEL FLOWMETER DOWNSTREAM TEMP.	TFL-2	I/C TC	X	X		
FUEL HEATER TEMPERATURE #1	TFH-1	I/C TC		X		
FUEL HEATER TEMPERATURE #2	TFH-2	I/C TC		X		
FUEL HEATER TEMPERATURE #3	TFH-3	I/C TC		X		
FUEL INJECTION TEMPERATURE	TFI	I/C TC	X	X		
FUEL INJECTION PRESSURE	PFI	TABER	X	X	X	
FUEL INJECTION KISTLER	PFIK	KISTLER			X	X
N_2O_4 (OXIDIZER) SYSTEM						
N_2O_4 TANK PRESSURE	POT	TABER		X		
OXIDIZER FLOWRATE #1	WOX-1	TURBINE FLOWMETER	X	X	X	
OXIDIZER FLOWRATE #2	WOX-2	TURBINE FLOWMETER	X	X	X	
OXIDIZER LINE TEMPERATURE	TOL	I/C TC	X	X		
OXIDIZER INJECTION TEMPERATURE	TOI	I/C TC	X	X		
OXIDIZER INJECTION PRESSURE	POI	TABER	X	X	X	
OXIDIZER INJECTION PHOTOCON	POIPH	PHOTOCON			X	X

TABLE 2 (Concluded)

INSTRUMENTATION LIST FOR HIGH ε TEST PROGRAM

PARAMETER/MEASUREMENT	SYMBOL	TRANSDUCER EMPLOYED	RECORDING SYSTEM			
			BECKMAN DIGITAL DATA SYSTEM	DIRECT READING RECORDER	OSCILLO-GRAPH	TAPE
THRUST CHAMBER						
CAVITY TEMPERATURES #1 THRU #7	TC-1 THRU TC-7	W/R TC**	X			
CHAMBER WALL TEMPERATURES #1	TCh-1 THRU TCh-24	C/A TC***	X	X(1)		
CHAMBER PRESSURE #1	PC-1	TABER	X	X		
CHAMBER PRESSURE #2	PC-2	TABER	X	X	X	X
THRUST	F	LOAD CELL	X	X		
CHAMBER KISTLER #1	PCK-1	KISTLER			X	X
CHAMBER KISTLER #2	PCK-2	KISTLER			X	X
CHAMBER KISTLER #3	PCK-3	KISTLER			X	X
MISCELLANEOUS						
WATER TEMPERATURE & WATER TANK	TW-WT	I/C TC		X		
WATER TEMP & WATER HEATER OUTLET	TW-WHO	I/C TC		X		
WATER TEMP & FUEL HEATER INLET	TW-FHI	I/C TC		X		
WATER TEMP & FUEL HEATER OUTLET	TW-FHO	I/C TC		X		
REFERENCE JUNCTION TEMPERATURE	RJT	I/C TC	X			
FUEL MAIN VALVES POWER & TRAVEL	---	------	X		X	
OXID. MAIN VALVE POWER & TRAVEL	---	------	X		X	X

*IRON/CONSTANTAN THERMOCOUPLE
**TUNGSTEN/RHENIUM THERMOCOUPLE
***CHROMEL/ALUMEL THERMOCOUPLE

TEST PROGRAM

The test program was conducted in four series; each series being characterized by a different hardware configuration. The conditions are summarized in Table 3.

TABLE 3

TEST CONDITIONS

Series	Tests	Primary (1T) Open Area %	Acoustic Cavities, Depth, Inches		Injector-to-Throat Length, Inches
			Physical*	Effective	
1	19-24	10	1.5	2.08	12
2	25	15	1.1	1.28	12
3	26-33	15	1.5	2.12	12
4	34-39**	15	1.5	2.12	12
5	40-46	10	1.5	2.08	16

*Depth from injector face
**Ambient Fuel Tests

Seven bombs were detonated during the first test series with no indication of instability. An erroneous RCC signal shutdown Test 23 (no bombs on this test) prematurely and the oxidizer valve closed early on Test 22. Test 25 was driven unstable by the first bomb so the cavity depth was increased for Test Series 3. This was the only instability encountered during the test program. Thirteen bombs were detonated during the third series without instabilities. The oxidizer valve again closed prematurely on Test 26. Performance was lower then anticipated leading to the suspicion that fuel

was leaking around the metal O-ring sealing the injector fuel manifold from the chamber. An elastomer O-ring was substituted for Test Series 4. The series was also conducted with ambient as well as hot fuel to determine the effect of this variable. An uninstrumented extension was installed between the instrumented spool and the chamber for Test Series 5 to determine the effect of chamber length on performance and thermal characteristics. The total duration accumulated during the program was approximately 108 seconds.

PERFORMANCE

Test conditions and performance parameters are summarized in Table 4. The redundant flowmeter and chamber pressure agreement was generally very good; and the performance values calculated from thrust and from chamber pressure agree well. The performance with the 12-inch chamber length appears to be insensitive to all operating conditions varied, i.e., chamber pressure, mixture ratio, and fuel temperature. A slight variation of performance with chamber pressure and mixture ratio was noted with the 16-inch length.

The variation of performance with length was approximately two percent for the 4-inch change in chamber length as shown in Fig. 7. A similar variation was observed with the L/D #1 injector in 8-inch diameter hardware. The performance of the L/D #1 with 2.7 percent (of total propellant) boundary layer coolant (BLC) was approximately 2.5 percent higher than that of the L/D #4 without BLC. The comparison is justified because the heat flux profile of the L/D #4 without BLC is lower than that of the L/D #1 with BLC as will be shown.

The L/D #4 injector was expected to have equal or greater performance than the L/D #1 based on the results of a subscale hot-firing test program. The results of the subscale tests are shown in Figs. 8 and 9. The data shown

TABLE 4

L/D #4 PERFORMANCE SUMMARY

Test	Dur Sec	$P_{C_{NS}}$, PSIA	F_{Site}, Pound	O/F	Total Flow, Lb/Sec	C^*_P Ft/Sec	C^*_F Ft/Sec	$\eta_{C^*_P}$ %	$\eta_{C^*_F}$ %	$\frac{C_F \text{ Meas.}}{\text{Pred.}}$
19	2.4	120.2	3199	1.645	19.4	5294	5225	92.7	91.5	.987
20	3.7	134	3698	1.844	21.46	5335	5257	93.5	92.2	.985
21	3.7	135.6	3751	1.542	21.75	5326	5269	93.5	92.5	.989
22	1.6	118.2	3133	1.734	18.92	5338	5269	93.5	92.3	.987
23	2	132.1	3624	1.674	21.24	5313	5245	93	91.9	.987
24	3.6	119.3	3170	1.653	19.18	5315	5250	93.1	91.9	.988
25	1.7	126.6	3440	1.664	20.37	5309	5254	93	92	.99
26	1.6	126.1	3432	1.656	20.16	5346	5302	93.6	92.9	.992
27	4.6	140.2	3944	1.797	22.5	5322	5276	93.2	92.4	.991
28	4.7	132.4	3668	1.437	21.37	5293	5280	93.1	92.9	.997
29	4.6	113.7	3005	1.825	18.37	5290	5254	92.7	92.1	.993
30	4.6	126	3440	1.624	20.34	5288	5263	92.7	92.2	.995
31	4.7	140	3938	1.609	22.53	5309	5278	92	92.5	.994
32	4.6	110	2874	1.484	17.8	5279	5277	92.8	92.7	.999
33	4.6	109.9	2862	1.63	17.77	5284	5259	92.6	92.1	.995
34	2.2	125.9	3387	1.669	20.25	5310	5233	93	91.6	.986
36	4.7	125.2	3384	1.622	20.17	5302	5254	92.9	92.1	.991
37	3.6	138.6	3867	1.86	22.41	5287	5212	92.7	91.4	.986
38	3.7	139.3	3886	1.636	22.48	5295	5241	92.8	91.8	.99
39	3.6	129.4	3529	1.424	20.95	5276	5237	92.9	92.2	.993
40	4.7	125.3	3444	1.692	19.61	5461	5471	95.6	95.8	1.002
41	4.7	140	3981	1.863	22.14	5404	5405	94.7	94.8	1
42	4.7	140	3964	1.545	22.1	5412	5422	95	95.1	1.002
43	4.7	111.6	3959	1.876	17.74	5375	5376	94.3	94.3	1
44	4.7	111.5	3942	1.71	17.69	5383	5394	94.5	94.5	1.002
45	4.7	126.5	3475	1.664	20.04	5394	5393	94.4	94.4	1
46	4.7	140.3	3958	1.704	22.25	5388	5366	94	94	.996

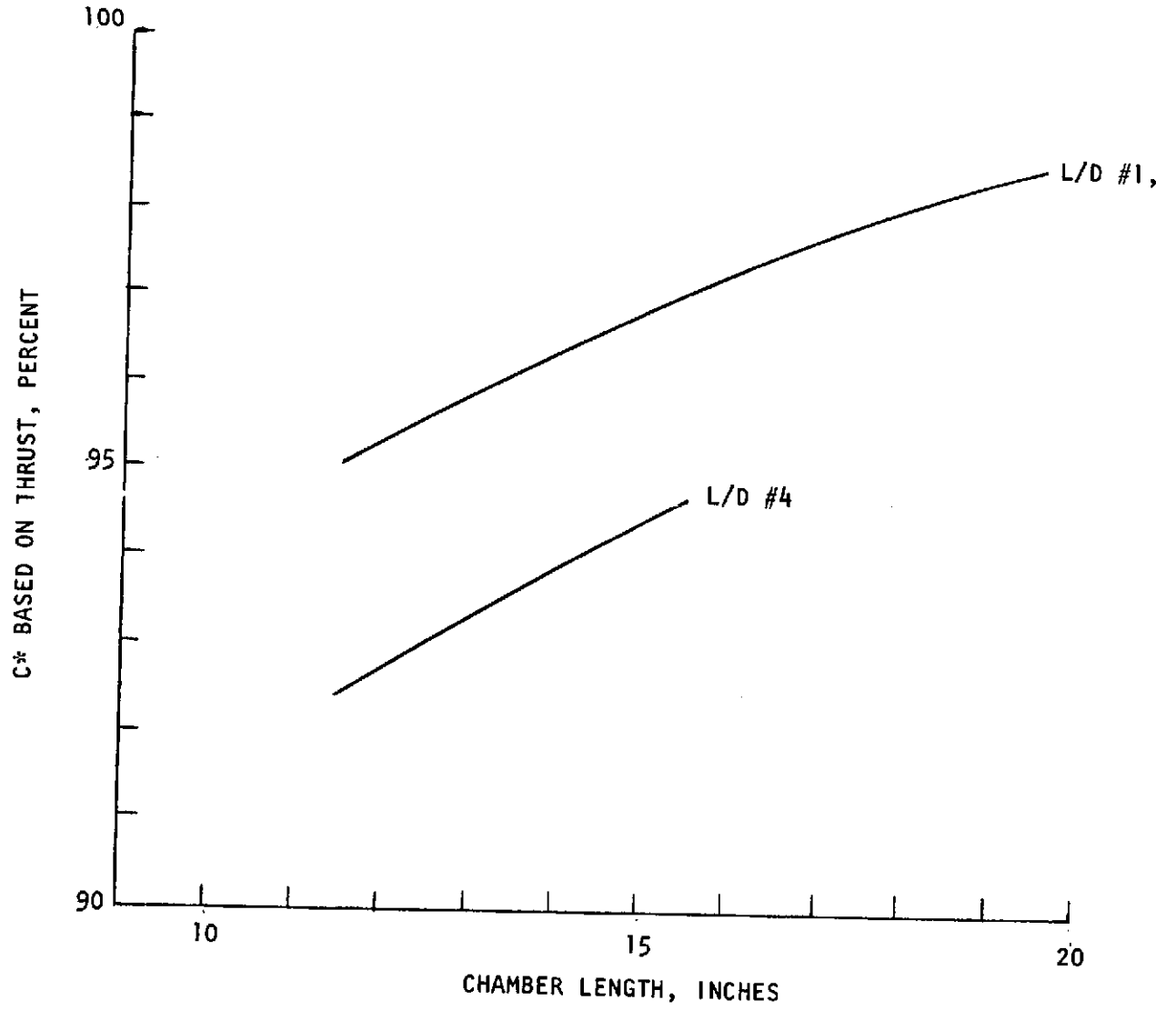

Figure 7. OME Like-Doublet Injector Performance

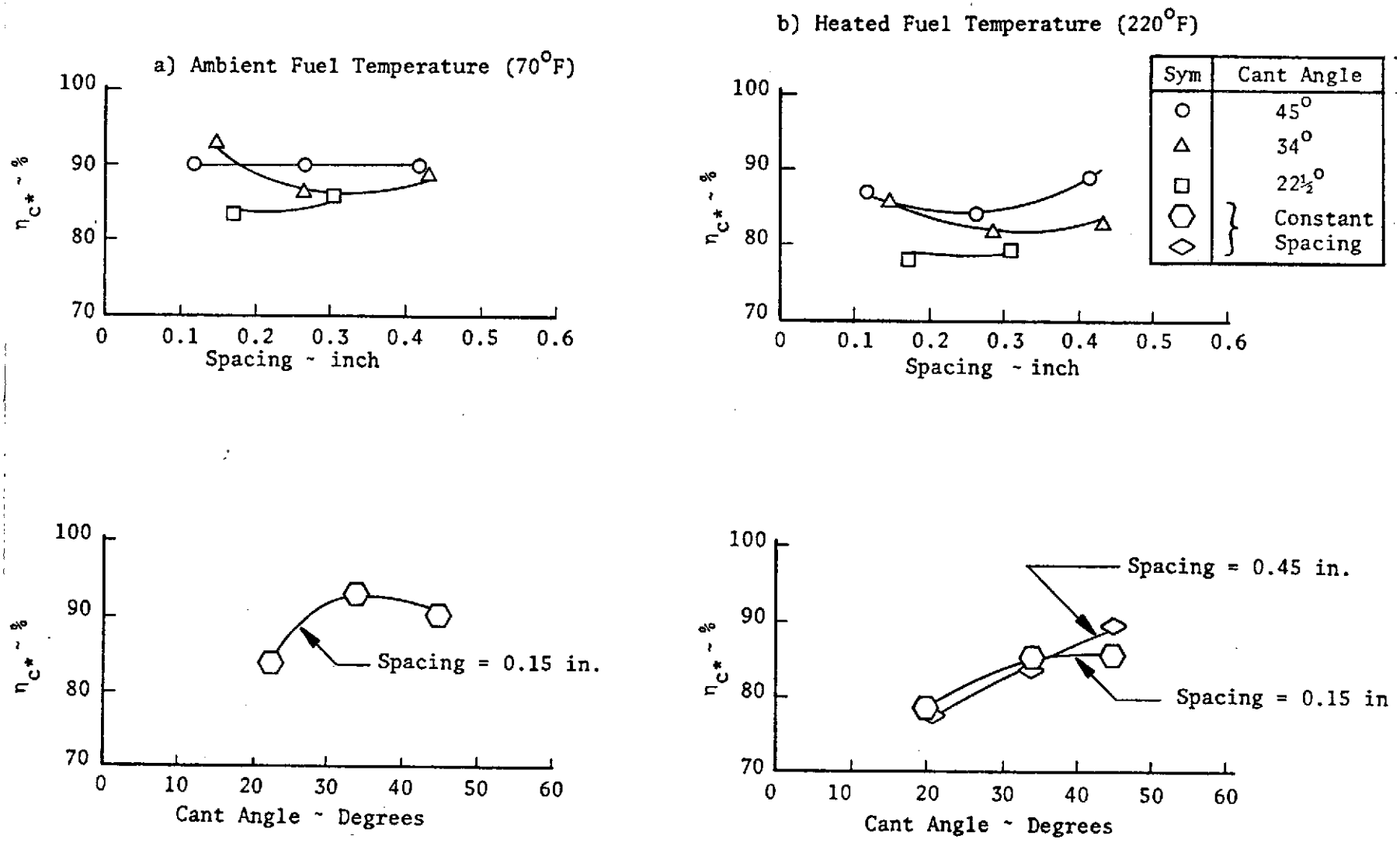

Figure 8. Subscale Test Results Element Geometry

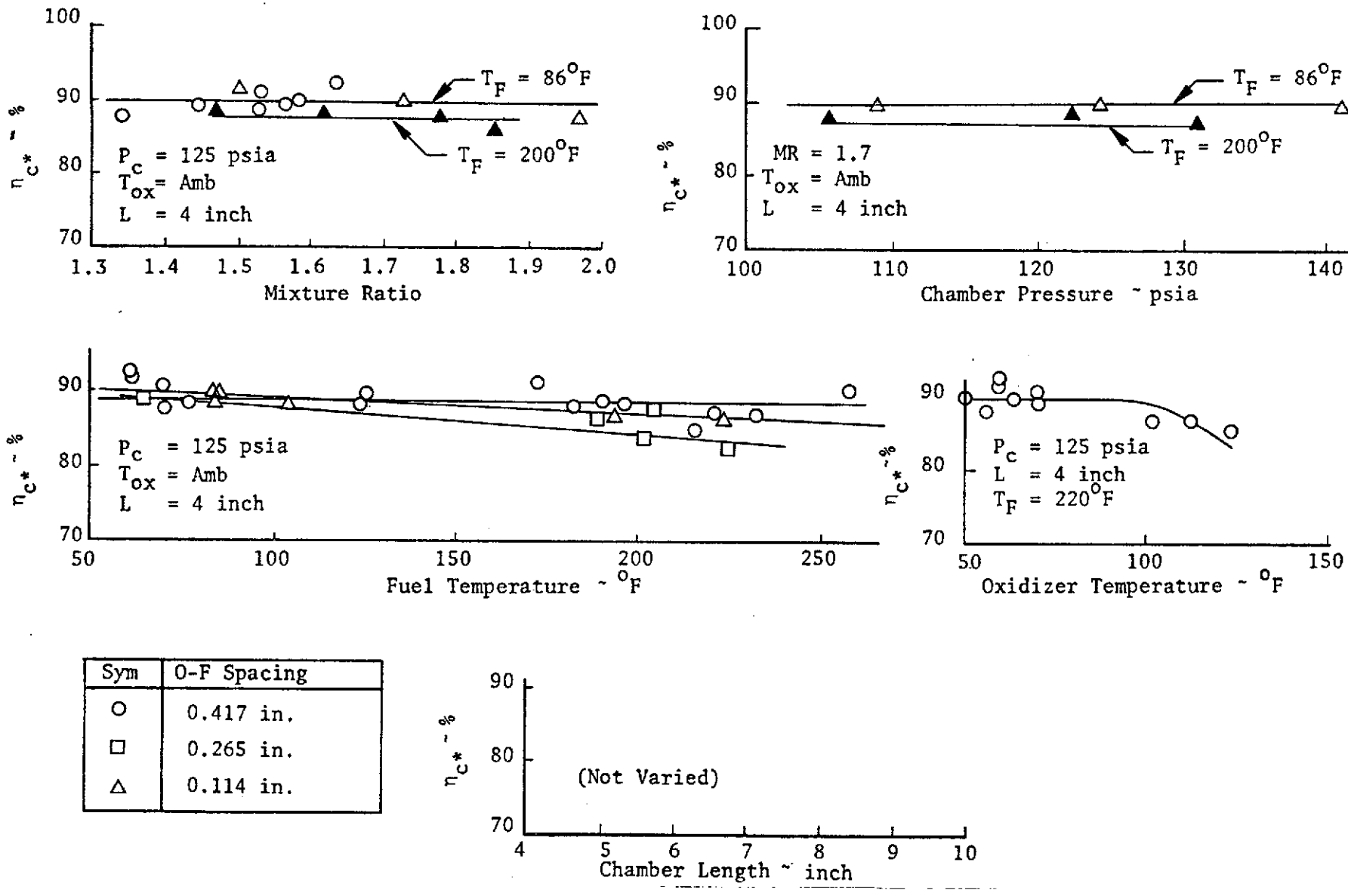

Sym	O-F Spacing
○	0.417 in.
□	0.265 in.
△	0.114 in.

Figure 9. Subscale Test Results Operating Condition

in Fig. 8 indicate that highest performance with hot fuel was obtained with a 0.45-inch spacing between the impingment points of the fuel and oxidizer jets and a total cant angle of 45 degrees. The data shown in Fig. 9 indicated the possibility of a slight performance decrease with increasing fuel temperature which is indicative of blowapart between the fuel and oxidizer fans.

A comparison of the significantly different parameters of the L/D #1 and L/D #4 injectors is shown in Table 5. The change in the element spacing and cant angle reflect the results of the subscale tests. The radial sequence of the impinging orifices was changed to an O-F-O-F configuration so that, if blowapart did occur, the unreacted propellant would be blown into a spray-field rich in the opposite propellant.

Three factors are potentially responsible for the lower performance of the L/D #4: blowapart, vaporization, and mixing. Blowapart is not likely because of the insensitivity of performance to fuel temperature indicated by the test data. The parallel nature of the two curves in Fig. 7 suggests similarity in vaporization efficiency characteristics. The implication is that the L/D #1 had a better mixing efficiency than the L/D #4. The element radial sequencing on the L/D #4 is such that any portion of the propellant fans which spray through each other tend to be in a region rich in the same propellant, thus, degrading the mixing efficiency. The wider element spacing also tends to make element fan mixing more sensitive to orifice mislocation.

The discharge coefficients based on total injector pressure drop are shown in Table 6. Coefficients for the orifices would be approximately one point (.01) higher because of the manifold pressure drop, calculated to be 1.5 psi. The low value of the oxidizer C_D may indicate poorly flowing orifices (perhaps because of the entrance being located too close to the wall).

TABLE 5

L/D #1 - L/D #4 COMPARISON

	LD #1	LD #2
INJECTOR DIAMETER, INCHES	8.2	10.0
NO. OF ELEMENTS	186	229
ELEMENT SPACING, INCHES	0.19	0.45
CANT ANGLE, DEGREES	22.5	45
RADIAL SEQUENCE	O-O-F-F	O-F-O-F

TABLE 6

L/D #4 INJECTOR PRESSURE DROP SUMMARY

Test	Dur Sec	$P_{C_{NS}}$, PSIA	F_{Site}, Pound	O/F	W_o lb/sec	P_o PSI	TIO F	C_{DOX}	W_F lb/sec	P_F PSI	TIF F	C_{DF}
19	2.4	120.2	3199	1.645	12.07	68	64	.667	7.34	49	186	.707
20	3.7	134.0	3698	1.844	13.92	91	64	.665	7.54	55	217	.693
21	3.7	135.6	3751	1.542	13.19	83	65	.664	8.55	70	210	.696
22	1.6	118.2	3133	1.734	12.00	67	63	.669	6.92	44	162	.700
23	2.0	132.1	3624	1.674	13.29	82	63	.669	7.94	59	180	.701
24	3.6	119.3	3170	1.653	11.95	68	63	.664	7.23	50	187	.694
25	1.7	126.6	3440	1.664	12.73	75	74	.676	7.65	54	189	.707
26	1.6	126.1	3432	1.656	12.57	75	76	.667	7.59	54	201	.702
27	4.6	140.2	3944	1.797	14.46	103	78	.656	8.04	61	192	.698
28	4.7	132.4	3668	1.437	12.60	77	82	.662	8.77	73	188	.696
29	4.6	113.7	3005	1.825	11.87	67	77	.669	6.50	40	189	.694
30	4.6	126.0	3440	1.624	12.59	75	66	.663	7.76	58	190	.687
31	4.7	140.0	3938	1.609	13.89	92	64	.662	8.64	71	185	.695
32	4.7	110.0	2874	1.484	10.63	54	60	.659	7.17	48	176	.696
33	4.6	109.9	2862	1.630	11.01	58	57	.660	6.76	43	188	.696
34	2.2	125.9	3387	1.669	12.66	75	62	.666	7.59	53	187	.707
36	4.7	125.2	3384	1.622	12.48	77	58	.647	7.69	51	70	.705
37	3.6	138.6	3867	1.860	14.57	105	62	.648	7.84	53	68	.701
38	3.7	139.3	3886	1.636	13.95	97	61	.645	8.53	63	65	.703
39	3.6	129.4	3529	1.424	12.31	76	58	.645	8.64	64	65	.703
40	4.7	125.3	3444	1.692	12.32	77	112	.658	7.28	52	225	.693
41	4.7	140.0	3981	1.863	14.40	102	108	.667	7.73	58	200	.689
42	4.7	140.0	3964	1.545	13.42	88	95	.662	8.68	73	194	.69
43	4.7	111.6	2959	1.876	11.57	64	78	.663	6.17	37	183	.683
44	4.7	111.5	2942	1.710	11.16	60	77	.664	6.53	42	194	.684
45	4.7	126.5	3475	1.664	12.52	75	75	.664	7.52	55	183	.687
46	4.7	140.3	3958	1.704	14.02	94	74	.664	8.23	66	198	.687

Flow sampling of the injector at various locations under back pressure (to prevent fully separate flow) would be required to ascertain mixture ratio distribution characteristics.

HEAT TRANSFER

Heat flux profiles for the L/D #4 injector based on chamber wall temperature are shown in Figs. 10 through 14 for the 12-inch chamber length. No supplementary BLC was provided. The profile at nominal operating conditions (Fig. 10) is considerably below the experimental profile for the L/D #1 with 2.5% BLC and the prediction for the L/D #4 (based on 97.5% C*) without BLC. The heat flux profile at high chamber pressure and nominal mixture ratio (Fig. 11) indicates very little effect of chamber pressure. This is in contrast with the results of tests on the L/D #1 injector which indicated that the total heat load was proportional to the 0.8 power of chamber pressure. The effect of mixture ratio is observed by comparing Figs. 11 and 12. The profile for O/F = 1.80 is approximately 10 percent higher than the profile for O/F = 1.61 which is a stronger dependency on mixture ratio than previously found with the L/D #1. Figure 13 is included to present data at low pressure and mixture ratio thus indicating the variation in the heat flux profile over the entire Pc - O/F range.

The effect of fuel temperature can be determined by a comparison of Figs. 10 and 14 ($\sim$190 F fuel was used for the tests from which the data for Figs. 10-13 were derived). The heated fuel increased the heat flux profile 5-10 percent in the cylindrical and early convergent portions of the chamber but had little effect further downstream. The heat flux values were reduced slightly by the addition of a 4-inch cylindrical section as indicated in the profile shown in Fig. 15.

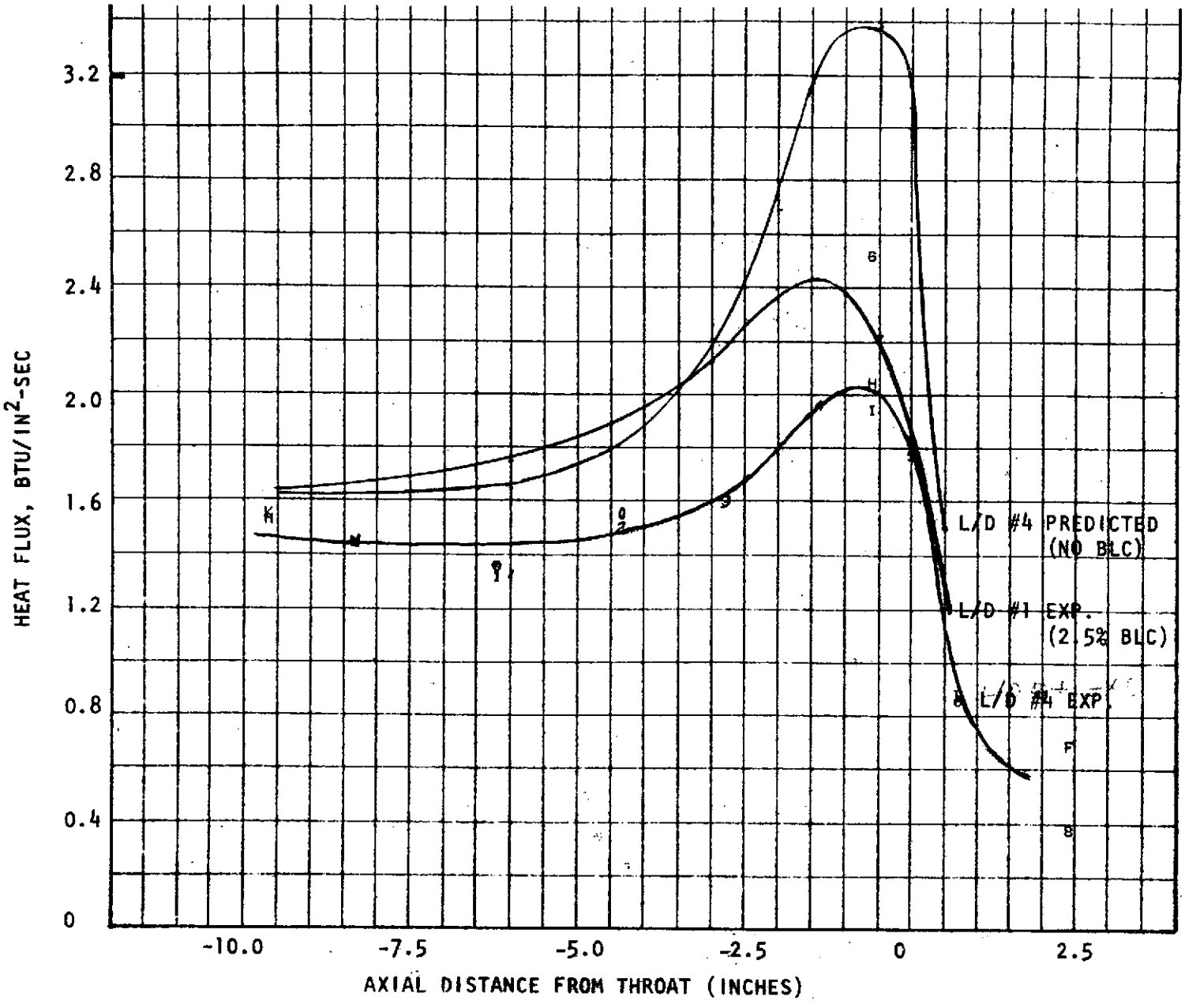

Figure 10. L/D #4 Test Thermal Results
Pc = 126 psia O/F = 1.62

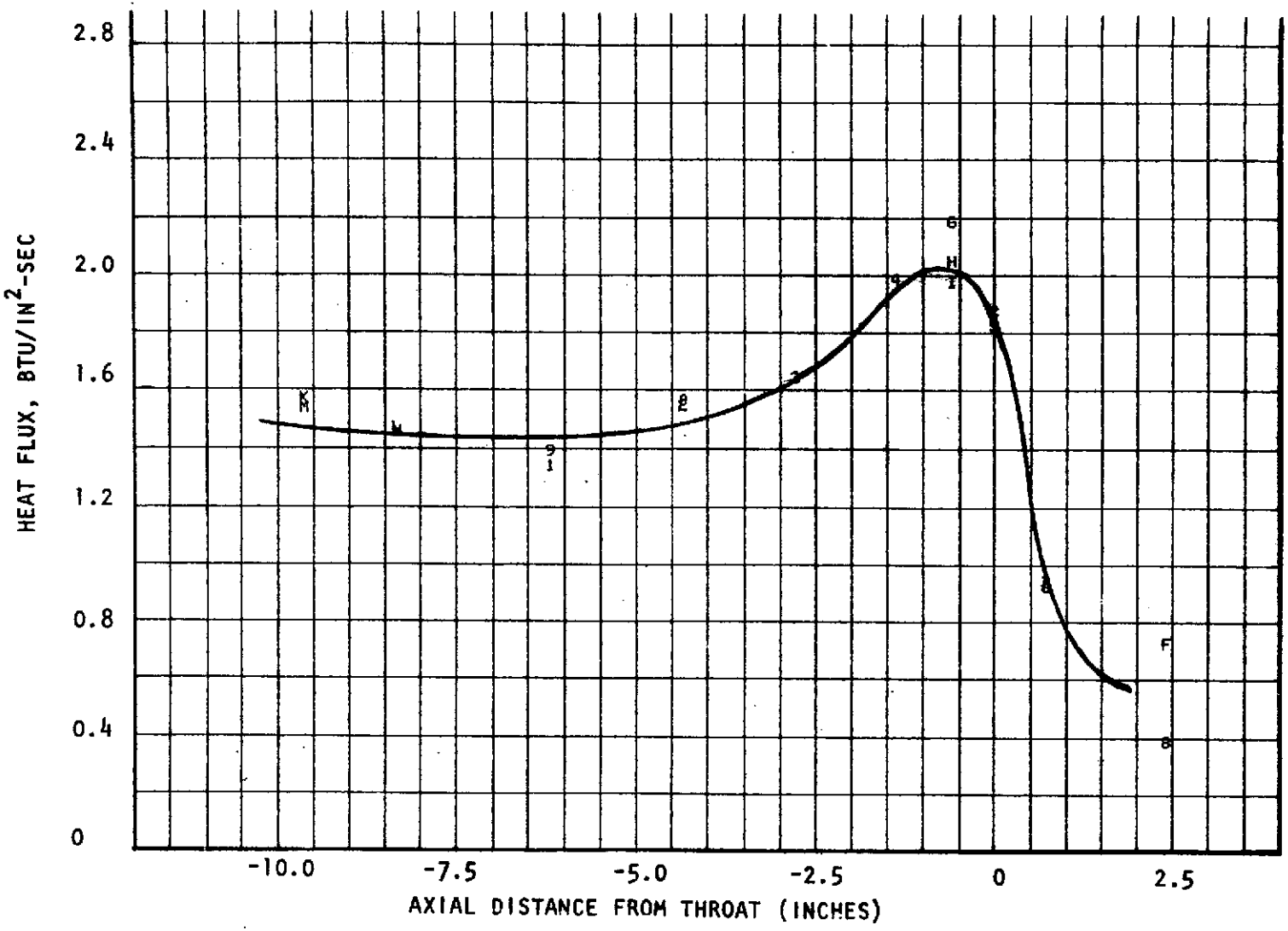

Figure 11. L/D #4 Test Thermal Results
Pc = 140 psia O/F = 1.61

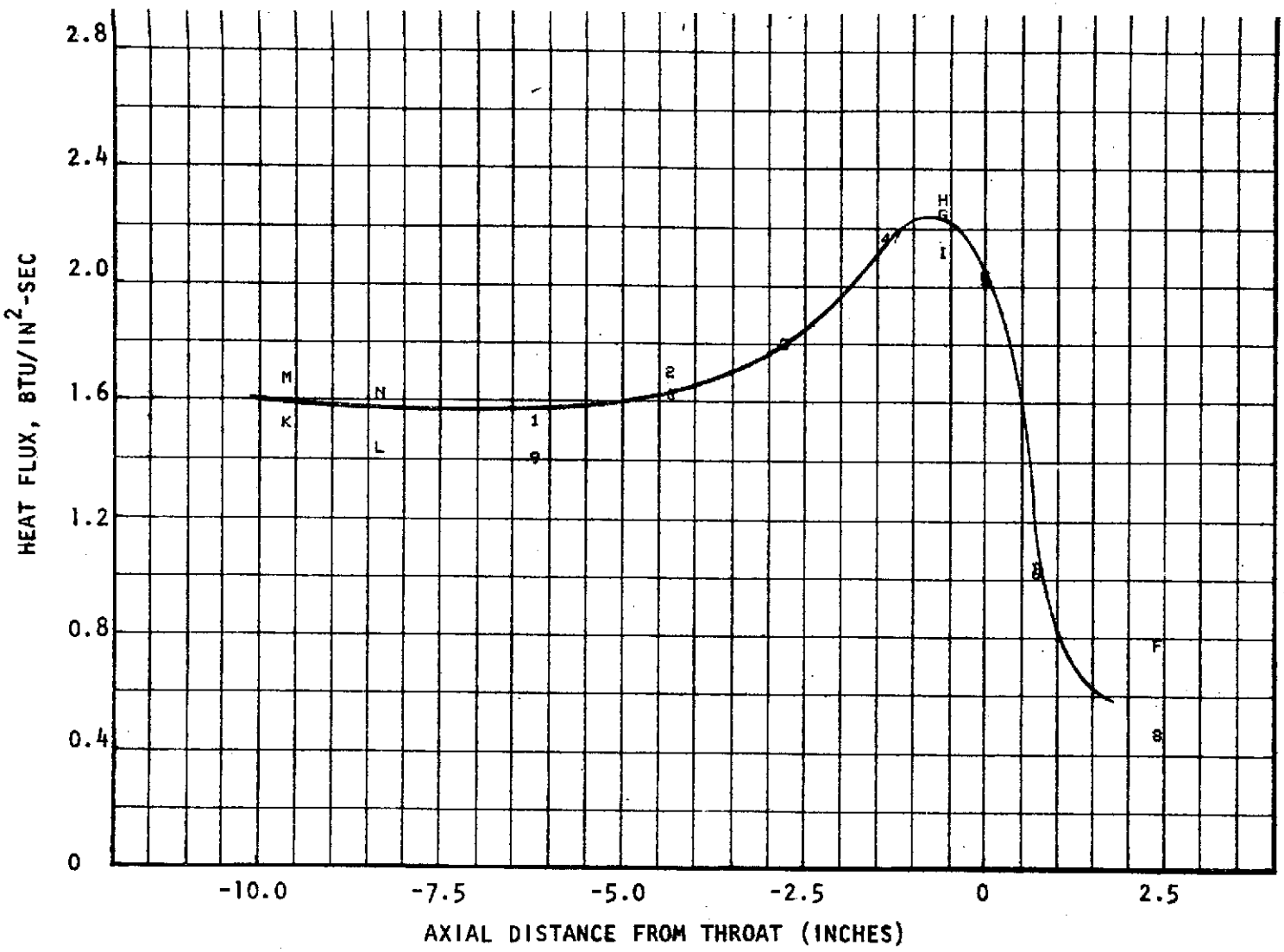

Figure 12. L/D #4 Test Thermal Results
Pc = 140 PSIA O/F = 1.80

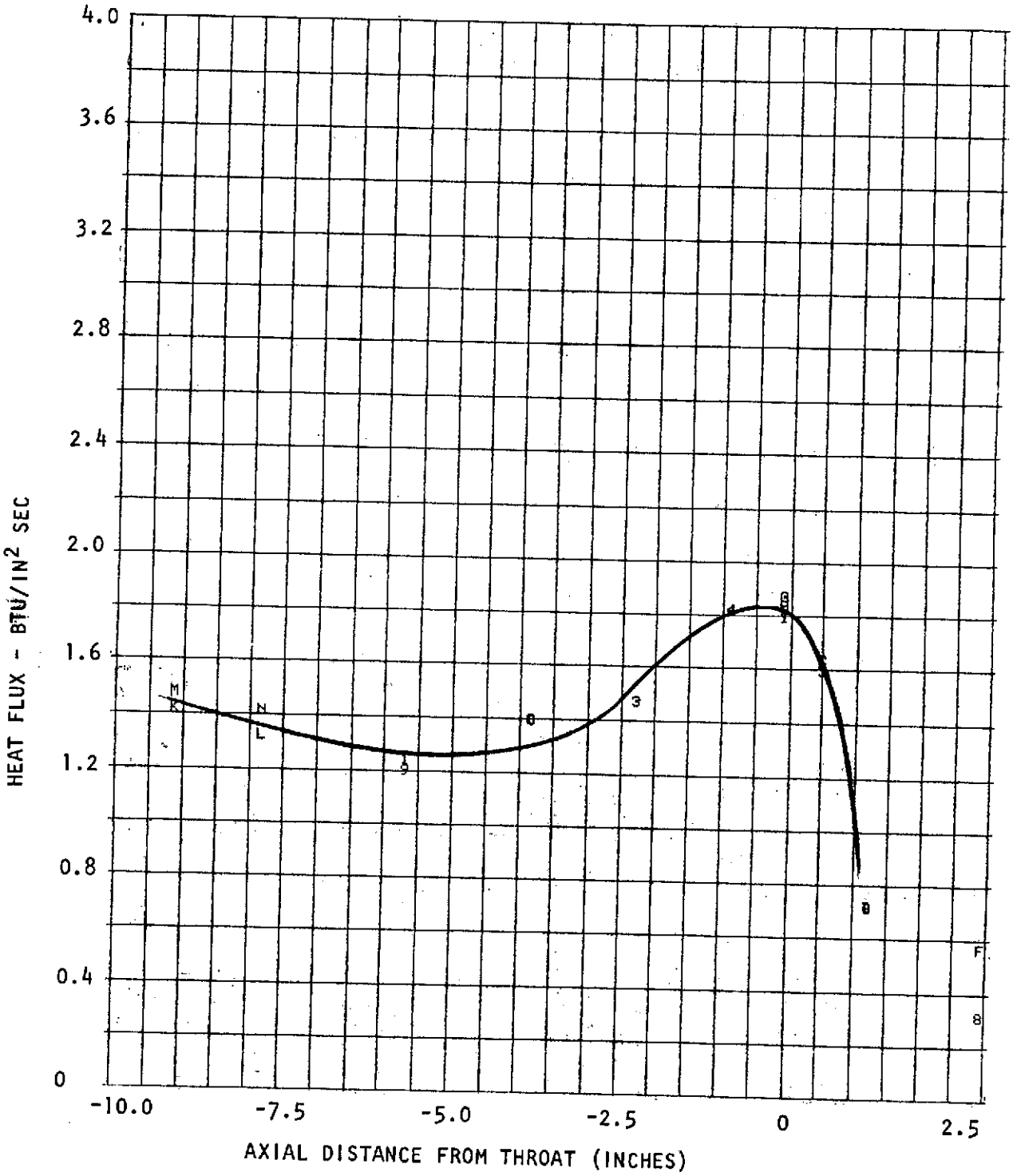

Figure 13. L/D #4 Thermal Results
Pc = 110 O/F = 1.48

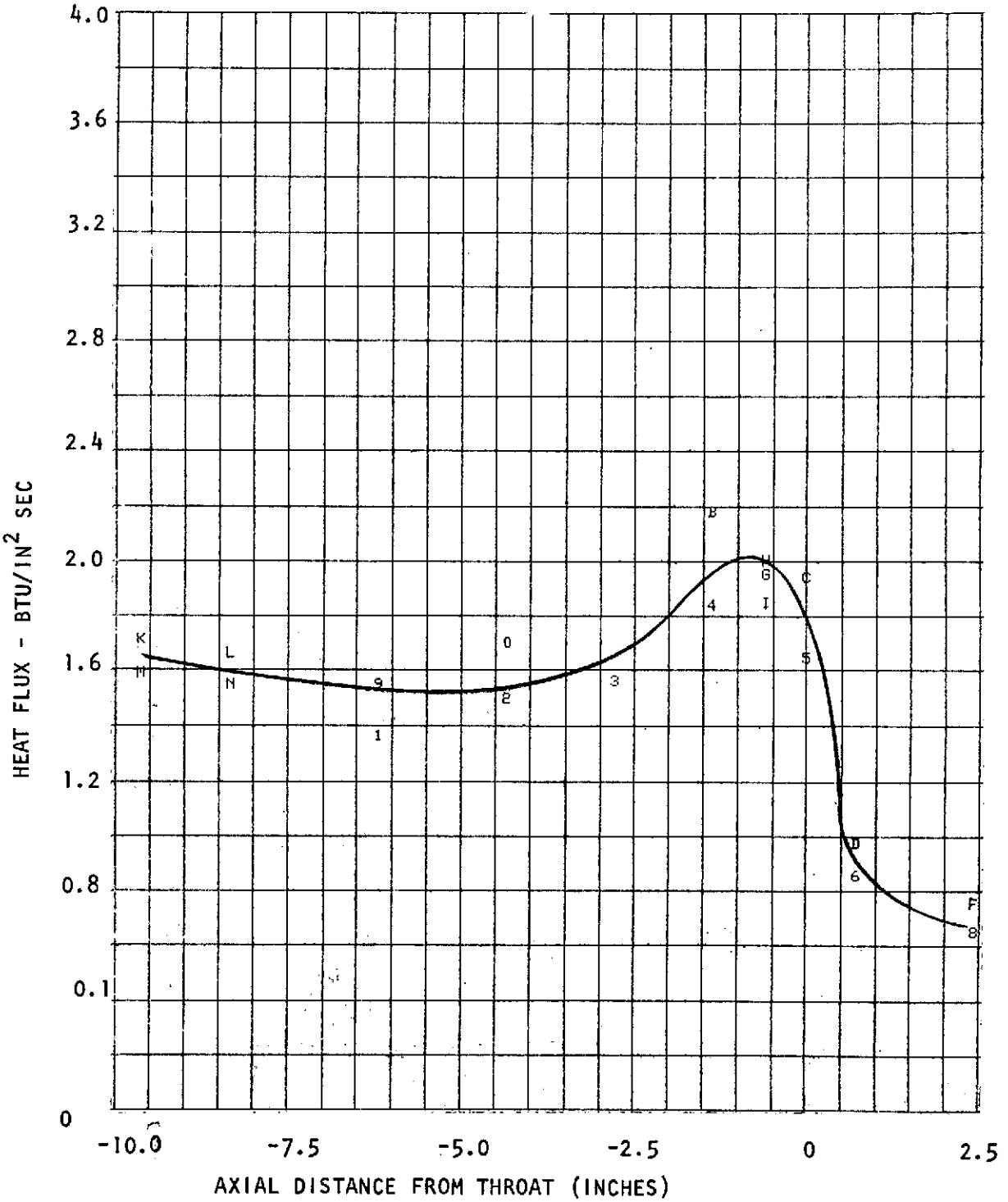

Figure 14. L/D #4 Thermal Results
Pc = 125 O/F = 1.62 Ambient Fuel

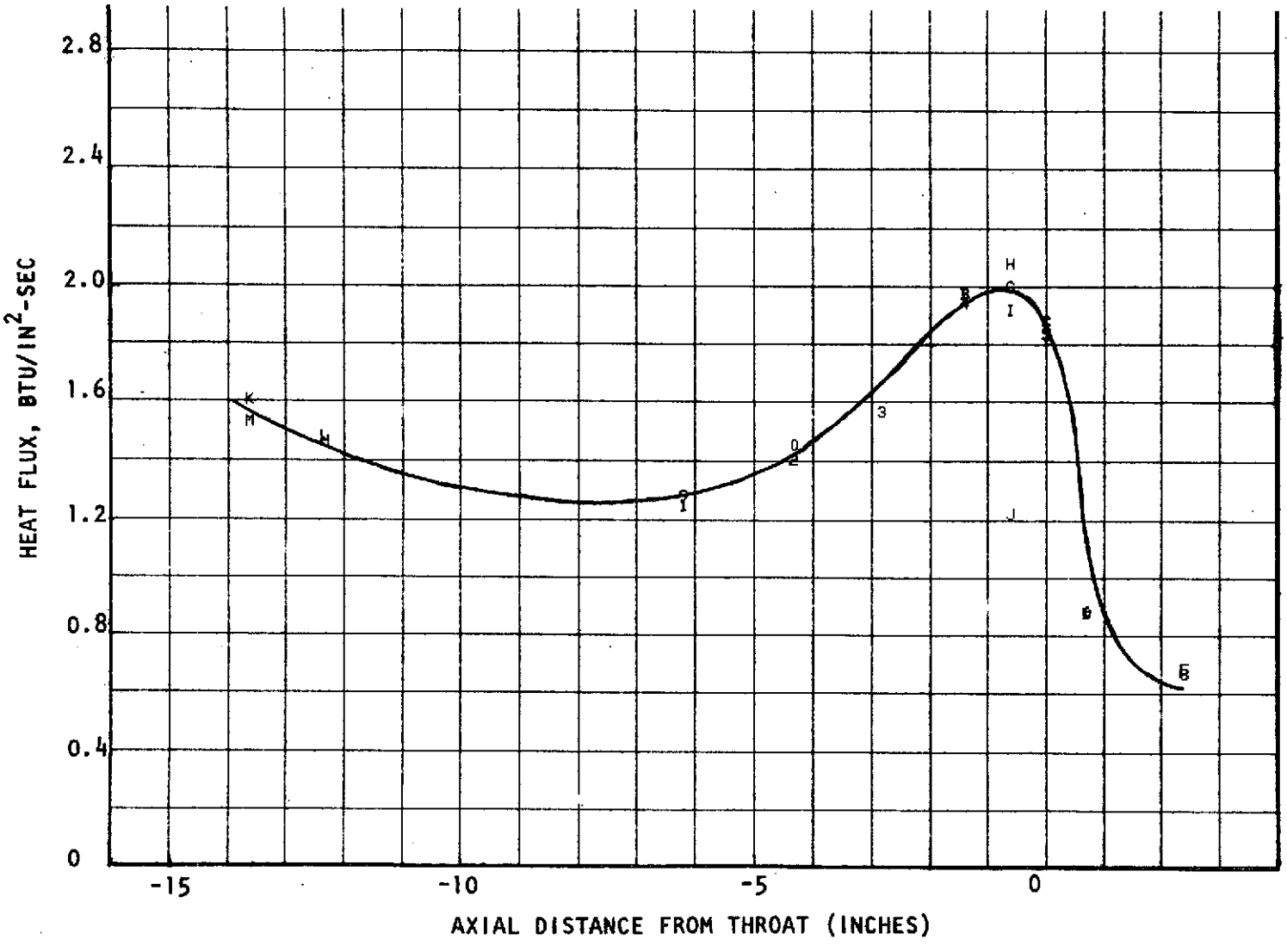

Figure 15. L/D #4 Test Thermal Results
Pc = 126 psia O/F = 1.67 Lc = 16 inches

The heat flux profiles were used to generate the heat load and subcooling data presented in Table 7. The heat load of the L/D #4 injector in a 12-inch long chamber without BLC is 88 percent of the load of the L/D #1 with BLC in a 14.7-inch long chamber, increasing the chamber length to 16 inches with the L/D #4 results in a heat load 8 percent higher and a subcooling 7 percent lower than the nominal L/D #1. Thus, the L/D #4 can be regeneratively cooled without requiring supplementary BLC.

Theoretically the heat flux would vary directly with η_c* so that a higher performing injector would result in only a slight increase in the heat load, i.e., an injector with 98 percent η_c* would result in a 3 percent increase in coolant pressure drop in a regenerative chamber. Actually, heat fluxes (particularly near the injector) tend to be more strongly affected by η_c* than the theoretical relationship suggests.

Acoustic cavity temperatures are shown in Table 8. The most significant effect is the variation of temperature with position in the cavity.

STABILITY

Stability results are summarized in Table 9. Each entry in the table corresponds to a single test with two bombs being used for each test, nominally. The cavity configurations were similar to those used in the 8.2-inch diameter chamber with contoured entrances and with 4 of 12 cavities tuned for the third tangential and first radial modes and 8 of 12 cavities tuned for the first tangential mode. The effective and physical depths of the secondary (3T/1R) cavity were 0.88 and 0.5 inches, respectively, for all tests. Testing was initiated with a 9.9 percent open area primary (1T) cavity (with effective and physical depths of 2.08 and 1.75 inches, respectively), which proved adequate to prevent instability.

TABLE 7

HEAT LOAD COMPARISON

INJECTOR	CHAMBER LENGTH (INCHES)	** HEAT LOAD (BTU/SEC)	NOMINAL* SUBCOOLING (F)
L/D NO. 1 - EXP. WITH BLC	14.7	720	158
L/D NO. 4 - PRED.	12.0	880	128
L/D NO. 4 - EXP.	12.0	631	175
L/D NO. 4 - EXP.	16.0	777	147

* W_F = 7.3 LB/SEC, PIF = 180 PSIA

** ADD $\approx$ 35 BTU/SEC FOR ACOUSTIC CAVITY COOLING

TABLE 8

ACOUSTIC CAVITY TEMPERATURES, F

Test	Pc psia	O/F	Thermocouple Number 1	2	5
40	125	1.69	1630	2630	
41	140	1.86	1600	2680	2560
42	140	1.55	1640	2660	2570
43	112	1.88	1660	2680	2650
44	112	1.71	1640	2690	2630
45	126	1.66	1640	2650	2600
46	140	1.70	1620	2650	2590
Cavity Type			1T	1T	1T
Depth from Inj. face, inches			0.6	-0.2	-0.2

TABLE 9

SUMMARY OF STABILITY RESULTS FROM HIGH CONTRACTION-RATIO CHAMBER TESTS

Objective	Primary Cavity (1) σ	Primary Cavity (2) ℓ_e, in.	Secondary Cavity (1) σ	Secondary Cavity (2) ℓ_e, in.	p_c, psia	Overall Mixture Ratio	Fuel Inj. Temp., F	Maximum Damp Time, msec	Frequency, Hz	Stability
Search for Minimum Open Area ↓	0.099 ↓	2.08 ↓	0.069 ↓	0.88 ↓	120	1.64	190	7		Stable ↓
					134	1.84	220	7		
					136	1.54	210	6		
					118	1.73	160	9		
Search for Minimum Depth	0.148	1.28			127	1.66	190	570	2640	Unstable
Confirm Stability at Nominal Depth ↓	0.148 ↓	2.12 ↓			126	1.66	201	6		Stable ↓
					140	1.80	192	6		
					132	1.44	188	6		
					114	1.82	189	7		
					126	1.62	190	6		
					140	1.61	185	5		
					110	1.48	176	7		
					126	1.67	187	8		
					-	-	-	8		
					125	1.62	70	8		
					139	1.86	68	7		
Confirm Stability with Long Chamber ↓	0.099 ↓	2.08 ↓	↓	↓	129	1.42	65	7		↓
					125	1.69	225	8		
					140	1.86	200	7		
					140	1.54	194	7		
					112	1.88	183	8		
					112	1.71	194	8		
					126	1.66	183	8		

(1) σ = Fractional open area based on injector face area.

(2) ℓ_e = Effective cavity depth.

However, a shallow 14.8 percent open area cavity was found to be inadequate. The latter cavity had an effective depth of 1.28 inches and a physical depth of 0.9-inch. Nevertheless, subsequent testing with a deeper 14.8 percent open-area cavity showed it to be adequate (physical depth of 1.75 inches).

The remaining tests were made, primarily, to evaluate the effects of fuel temperature and chamber length on steady-state performance. The combustion chamber was stable during all remaining tests.

Results from the stability testing show that adequate stability was readily achieved with a contoured entrance cavity without overlap. However, the stability is influenced, to some extent, by the lower performance.

CONCLUSIONS

Testing of the L/D #4 injector has demonstrated:

1. Thermal heat loads similar to that of the L/D #1, 8-inch diameter injector with a lower injector-end heat flux level. The injector, without boundary layer coolant, is compatible with the regenerative cooling concept.

2. The performance of the injector, η_c*, was lower than anticipated (95 percent in a 16-inch long chamber). Arrangement of the elements or orifice hydraulics are probably responsible.

3. The injector was stable with an acoustic cavity configuration readily adaptable to a regeneratively cooled thrust chamber. The injector can be stabilized with primary acoustic cavities having contoured inlets and 9.9 percent open area.

RECOMMENDATION

Hydraulic tests should be undertaken to further establish the flow and mixing characteristics of the injector. Individual orifice flows and mixture ratio distribution should be determined with the injector flowing water under normal back pressure. Additional analysis and tests should be conducted to improve the performance of this type injector.